Journal of Solid State Chemistry **167,** 168–181 (2002)
doi:10.1006/jssc.2002.9639

Crystal Structure Approach of the Disordered New Compounds $Bi_{\sim 1.2}M_{\sim 1.2}PO_{5.5}$ (M=Mn, Co, Zn): The Role of Oxygen-Centered Tetrahedra Linkage in the Structure of Bismuth–Transition Metal Oxy-phosphates

F. Abraham,*[,1] O. Cousin,* O. Mentre,* and El M. Ketatni†

*Laboratoire de Cristallochimie et Physicochimie du Solide, UPRESA CNRS 8012, ENSCL, Université des Sciences et Technologies de Lille, B.P. 108, 59652 Villeneuve d'Ascq Cedex, France; and †Laboratoire d'Electrochimie et Chimie des Matériaux, Faculté des Sciences, Université Cadi Ayyad, B.P. 523, Beni Mellal, Morocco

Received January 8, 2002; in revised form April 12, 2002; accepted May 3, 2002

The crystal structures of some recently published bismuth–transition metal oxy-phosphates are described as the association of complex infinite one-dimensional polycations and phosphate anions. The complex cations are built from oxygen-centered tetrahedra sharing edges to form infinite ribbons of *n* tetrahedra width. This structural concept allows one to describe the essential structural features of new highly disordered bismuth–transition metal oxy-phosphates, $Bi_{\sim 1.2}M_{\sim 1.2}PO_{5.5}$ (M = Mn, Co, Zn). The new compounds have been synthesized and structurally characterized by single-crystal X-ray diffraction. The three compounds crystallize in the orthorhombic space group *Ibam* (No. 72), $Z = 8$. The lattice parameters are $a = 15.079(2)$, $b = 11.247(2)$, $c = 5.437(1)$ Å for M = Mn, $a = 14.752(3)$, $b = 11.205(3)$, $c = 5.434(2)$ Å for M = Co and $a = 14.809(2)$, $b = 11.214(1)$, $c = 5.440(1)$ Å for M = Zn. Because of a high disorder over several cationic sites, only an approach of the crystal structure determination has been achieved. Actually, the structure is characterized by perfectly defined ribbons parallel to the (010) plane and built from a central chain of edge-shared OBi_4 tetrahedra running along the *c* axis and linked by edges to two other edge-shared $O(Bi,M)_4$ tetrahedra chains. The positions at the border of ribbons are randomly occupied by bismuth and M atoms. The formula of the three tetrahedra width ribbons is $(O_3Bi_{2.4}M_{1.6})^{+4.4}$. The phosphate ions and M^{2+} cations are disordered in the interspace between the ribbons. © 2002 Elsevier Science (USA)

INTRODUCTION

These last years, several bismuth-based oxy-phosphates and oxy-vanadates were synthesized and characterized from a structural point of view essentially by Sleight's group (1–6) and our group (7–14). They answer the formulations $BiMPO_5$ (M = Ni, Co) and BiM_2XO_6 (M being a divalent metal and X = P, V, As). The structures were described in a classic way using the association of oxygenated polyhedra around the cations. Owing to the Bi^{3+} lone pair stereoactivity, these materials frequently crystallize in noncentrosymmetric space groups enabling potential ferroelectric or nonlinear optical properties. Within that frame, $BiPb_2VO_6$ was recently investigated (15) and appeared to adopt the acentric *Pn* space group (16). More recently, we obtained new oxy-phosphates of bismuth and transition metals $Bi_{\sim 1.2}M_{\sim 1.2}PO_{5.5}$ with M = Mn, Co, Zn, which exhibit complex structural disorders avoiding a clear imaging of the network. The use of a crystallographic–chemical concept, fluorite based, privileging the tetrahedral environment of oxygen atoms not belonging to the phosphate groups allows us to describe these structures as resulting from the assembly of PO_4^{3-} ions and complex cations formed by the linkage of $O(Bi, M)_4$ oxygen-centered tetrahedra through edges.

In this paper, we report the preparation and the crystal structure approach of these new oxy-phosphates. A review of a number of materials matching this new description concept will be given, enabling the building of complex cations going from the mono-dimensional chain, with a one tetrahedron width, until the infinite $Bi_2O_2^{2+}$ two-dimensional layers of Aurivillius's phases by progressive 2, 3,… tetrahedra linkage.

EXPERIMENTAL

Syntheses

Several Bi–*M*–P–O (M = Mn, Co, Zn) compositions including titled compounds were prepared by solid-state

[1] To whom correspondence should be addressed. Fax: 33-03-20-43-68-14. E-mail: abraham@ensc-lille.fr.

0022-4596/02 $35.00

TABLE 1
Crystal Data, Intensity Measurement, and Structure Refinement Parameters for $Bi_{1.2}M_{1.2}PO_{5.5}$ (M = Mn, Co) Single Crystals

Formula	$Bi_{1.2}Mn_{1.2}PO_{5.5}$	$Bi_{1.2}Co_{1.2}PO_{5,5}$
Crystal symmetry	Orthorhombic	Orthorhombic
Space group	*Ibam*	*Ibam*
Lattice parameters (Å)[a]	$a = 15.079(2)$	$a = 14.752(3)$
	$b = 11.247(2)$	$b = 11.205(3)$
	$c = 5.437(1)$	$c = 5.434(2)$
Volume (Å^3)	922.1(5)	898.3(8)
Z	8	8
Equipment	Nonius CAD4	PhilipsPW1100
λ Mo$K\alpha$ (graphite monochromator)	0.7107 Å	0.7107 Å
Scan mode	ω–2θ	ω–2θ
Scan width (θ) (deg)	0.9	1.6
θ range (deg)	2–35	2–35
Recording reciprocal space	$-24 \le h \le 24$	$-24 \le h \le 24$
	$-18 \le k \le 18$	$-18 \le k \le 18$
	$0 \le l \le 8$	$0 \le l \le 8$
Number of measured reflections	4398	4300
Number of reflections $I > 3\sigma(I)$	2908	2325
Number of independent reflections	849	684
Standard reflections	$\bar{4}\bar{3}1$, 002, $\bar{3}2\bar{1}$	002, $0\bar{4}0$, $23\bar{1}$
	$1\bar{1}0$	$1\bar{1}0$
	$\bar{1}10$, 0.020	$\bar{1}10$, 0.015
Limiting faces and distances	110	110
(mm) between faces	$\bar{1}\bar{1}0$, 0.029	$\bar{1}\bar{1}0$, 0.036
	001	001
	$00\bar{1}$, 0.200	$00\bar{1}$, 0.170
μ (cm^{-1}) ($\lambda K\alpha = 0.7107$ Å)	459.0	479.4
Transmission factor range	0.232–0.435	0.183–0.394
Merging factor (R_{int})	0.032	0.067
Number of refined parameters	59	57
$R = \sum[\|F_o\| - \|F_c\|]/\sum\|F_o\|$	0.061	0.082
$R_w = [\sum w(\|F_o\| - \|F_c\|)^2 // \sum wF_o^2]^{1/2}$ with $w = 1/s(F_o)$	0.077	0.091

[a] Values refined from powder X-ray diffraction.

reactions of Bi_2O_3 (Aldrich, 99.9%), CoO (Aldrich, 99%), ZnO (Cerac, 99.9%) or MnO_2 (Aldrich) and $(NH_4)_2HPO_4$ (Fluka, puriss). Weighted mixtures of the three components were ground in an agate mortar and placed into a gold crucible. First, the mixtures were fired at 300°C for 2 h to decompose $(NH_4)_2HPO_4$. They were then ground and reheated at 500°C for 2 h in air and quenched to room temperature. The reaction was achieved after a final regrinding and heating at 850°C for 48 h.

Crystal growth of the cobalt compound was carried out from a nonstoichiometric mixture corresponding to the proportion Bi:Co:P = 2:2:1. For the Mn and Zn compounds, the starting mixtures correspond to the composition Bi:M:P = 1:1:1. The mixtures were submitted to the same thermal processing as that for the powder preparation. They were finally melted at 950°C, 975°C and 900°C for Co, Mn and Zn, respectively, and cooled down at 3°C/h to room temperature. For M = Co, three kinds of crystals were isolated from the inhomogeneous product: black octahedral crystals identified as Co_3O_4, colorless plate-like crystals of already described $Bi_{6.67}P_4O_{20}$ (17) and purple needle-shaped crystals with orthorhombic unit cell corresponding to the compound detailed in the present paper. Brown and white needle-shaped single crystals were isolated from the melt for M = Mn and Zn, respectively. A preliminary study of the selected crystals indicated the same symmetry and unit cell parameters comparable for the three metals. For the Zn compound, the poor quality of the single crystal did not allow to refine the structural parameters.

Microcrystalline powders were characterized by X-ray diffraction techniques using a Siemens D5000 goniometer equipped with a graphite back-monochromator, Cu$K\alpha$ radiation. The unit cell parameters refinement was performed from XRD collected in the 5–100° 2-θ range (0.02° step, 10 s counting time). Densities were measured using a Micromeritics Accupyc 1330 helium pycnometer. An elemental analysis was performed on $Bi_{1.2}Mn_{1.2}PO_{5.5}$ single crystals using an Environmental Scanning Electron Microscope Electroscan OXFORD 2020 equipped with an energy dispersive spectroscopy (EDS) detector. The magnetization was collected on heating from 5 K to room temperature using a Faraday balance magnetometer with an applied field of 0.12 T for $Bi_{1.2}M_{1.2}PO_{5.5}$ with M = Mn and Co.

The single crystal data collections were performed using a CAD-4 Enraf-Nonius or a Philips PW1100 diffractometer (Mo$K\alpha$ radiation). Lorentz polarization corrections and faces-indexed-based absorption corrections (18) were applied. Experimental details pertaining to the data collection and refinement results are given in Table 1. Atomic scattering factors (19) were corrected for anomalous dispersion (20). The full-matrix least-squares

TABLE 2
Atomic Coordinates and Displacement Parameters for $Bi_{1.2}Mn_{1.2}PO_{5.5}$

Atom	Site	Occupancy	x	y	z	B (Å^2)
Bi(1)	8j	1	0.09260(6)	0.10846(8)	0	1.22(2)
Bi/M(1)	8j	0.15(1)/0.85	0.2349(2)	0.4055(3)	0	2.27(8)
O(1)	4a	1	0	0	$\frac{1}{4}$	1.4(4)
O(2)	8f	1	0.179(1)	0	$\frac{1}{4}$	1.4(3)
Mn(2)	16k	0.10(1)	0.001(2)	0.426(2)	0.057(4)	0.9(5)
Mn(3)	4b	0.42(4)	$\frac{1}{2}$	0	$\frac{1}{4}$	6.5(1.1)
P(1)	8j	0.47(4)	0.351(1)	0.196(2)	0	2.0(4)
P(2)	16k	0.22(2)	0.105(1)	0.661(2)	0.057(3)	1.0(4)
O(3)	8j	0.47	0.435(5)	0.281(6)	0	4.2(1.3)
O(4)	16k	0.47	0.310(3)	0.222(4)	0.250(9)	3.8(8)
O(5)	8j	0.47	0.366(3)	0.076(5)	0	2.6(8)
O(6)	8j	0.44	0.388(3)	0.294(4)	0	1.7(7)
O(7)	16k	0.22	0.109(4)	0.363(6)	0.190(13)	2.2(1.0)
O(8)	16k	0.22	0.178(5)	0.599(7)	−0.123(15)	2.7(1.2)
O(9)	16k	0.22	0.022(3)	0.612(5)	−0.029(15)	1.5(9)

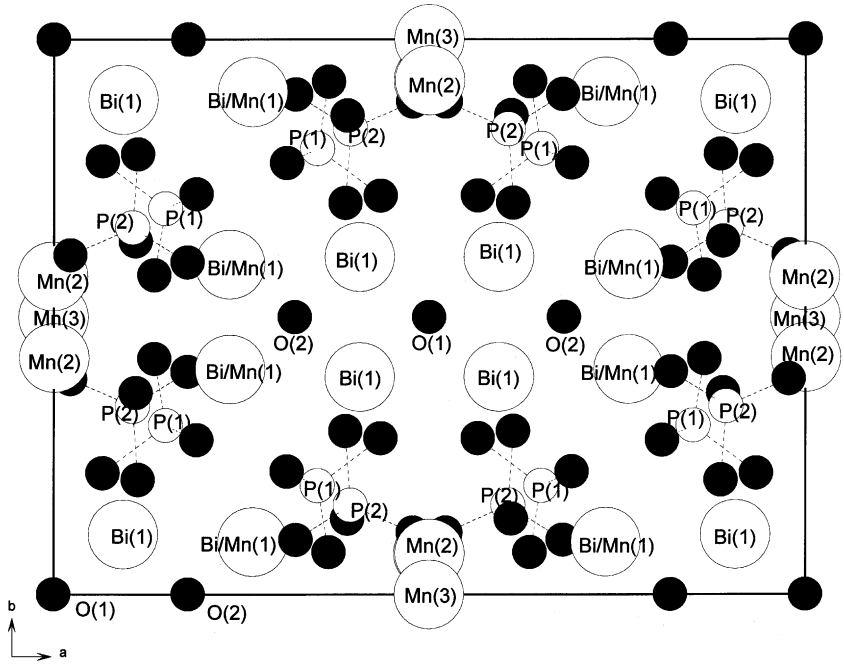

FIG. 1. Projection of the structure of $Bi_{1.2}Mn_{1.2}PO_{5.5}$ along the [001] direction showing the labeled scheme. For clarity, phosphate group oxygens are not labeled.

refinements were performed with a local modification of the SFLS-5 program (21).

STRUCTURAL APPROACH

The mean structure of $Bi_{\sim 1.2}M_{\sim 1.2}PO_{5.5}$ with $M = Mn$, Co, Zn was determined by X-ray single-crystal diffraction methods. Weissenberg diagrams and diffractometer studies indicate that these compounds crystallize in the orthorhombic system with extinctions indicating space groups *Iba2* or *Ibam*. No superstructure spots were observed. The crystal structure determination approach was carried out in the centrosymmetric space group *Ibam* (No. 72).

For clarity reasons, the structural approach performed for the manganese compound will be described as follows. First, bismuth atoms were located in an (8*j*) site using the Patterson function calculation. The manganese, phosphorus and oxygen atoms were subsequently located in positions Mn(1), P(1), O(1) and O(2) (Table 2 and Fig. 1) by the Fourier difference synthesis calculation. After refinement of the corresponding atomic coordinates and isotropic displacement parameters, various difficulties appear at this stage of study. Then, maxima of electronic density appear on the Fourier difference synthesis in the neighborhood of Mn(1)'s position, so this position was split into two close (8*j*) sites partially occupied by Bi and Mn atoms, respectively. Second, a maximum was also observed at a (16*k*) position which is then partially occupied by a manganese atom, Mn(2). Finally, the displacement parameter for the phosphorus atom is too high ($6.5\,Å^2$) and another (16*k*) site appeared, also occupied by phosphorus P(2); the occupancies of the two partially occupied phosphorus sites are refined. Finally, considering anisotropic thermal displacements for the

TABLE 3
Formulae Deduced from the Structural Approach at Different Stages of the Treatment[a]

	Mn compound		Co compound	
Stage	Formula	R/R_w	Formula	R/R_w
1	$Bi_{1.12}Mn_{1.18}(PO_4)_{1.00}O_{1.5}$	0.077/0.099	$Bi_{1.17}Co_{1.16}(PO_4)_{1.15}O_{1.5}$	0.092/0.108
2	$Bi_{1.13}Mn_{1.29}(PO_4)_{1.01}O_{1.5}$	0.074/0.094	$Bi_{1.18}Co_{1.25}(PO_4)_{1.24}O_{1.5}$	0.089/0.101
3	$Bi_{1.14}Mn_{1.18}(PO_4)_{0.84}O_{1.5}$	0.070/0.087	$Bi_{1.17}Co_{1.25}(PO_4)_{0.90}O_{1.5}$	0.090/0.101
4	$Bi_{1.15}Mn_{1.26}(PO_4)_{0.91}O_{1.5}$	0.061/0.077	$Bi_{1.18}Co_{1.31}(PO_4)_{1.02}O_{1.5}$	0.082/0.091

[a] 1: Oxygens of phosphate groups and $M(3)$ are not introduced; 2: $M(3)$ introduction (no phosphate groups oxygen atoms); 3: phosphate groups oxygen atoms but no $M(3)$; 4: all atoms.

TABLE 4
Unit Cell Parameters and Density Values for the $Bi_{1.2}M_{1.2}PO_{5.5}$ (M = Mn, Co, Zn) Compounds

M	a (Å)	b (Å)	c (Å)	V (Å^3)	F_{20}	ρ_{mes}.(g cm^{-3})	ρ_{cal}.(g cm^{-3})
Mn	15.079(2)	11.247(2)	5.437(1)	922.1(5)	140(0.0042, 34)	6.27(1)	6.28
Co	14.752(3)	11.205(3)	5.434(2)	898.3(8)	151(0.0039, 34)	6.43(1)	6.51
Zn	14.809(2)	11.214(1)	5.440(1)	903.4(4)	140(0.0042, 34)	6.52(1)	6.59

bismuth atoms and the Mn(1) site, the two (8*j*) positions partially occupied by Bi and Mn(1) get closer and can be gathered on one unique mixed Bi/Mn(1) site. The refinement of the occupancies for the mixed Bi/Mn site and for Mn(2), P(1) and P(2) sites yielded, at this stage, the formula $Bi_{1.12}Mn_{1.18}P_{1.0}O_{1.5}$ with $Z = 8$. The structural approach for the Co compound was performed in the same way and the met difficulties were comparable. With the same refinement conditions the formula deduced from the structural approach is $Bi_{1.17}Co_{1.16}P_{1.15}O_{1.5}$. A new difference synthesis revealed a maximum corresponding to (4*b*) and (8*i*) sites for the Mn and Co compounds, respectively. Whatever the chemical nature of the element occupying the corresponding positions, the atomic displacement is very large. For the Mn compound this site, Mn(3), is located at the center of a square formed by four Mn(2) atoms, for the Co compound it is distributed on both sides from the center. Partial occupation of this site by M atoms led to the formulae reported in Table 3. The introduction of oxygen atoms of phosphate groups located from a last difference synthesis with occupancies and isotropic displacement parameters fixed to the values of phosphorus atoms to which they are bound generates a weak decrease of the occupancy of phosphorus (Table 3). The results of the structural approach are reported in Table 2 for the Mn compound in the case of hypothesis 4 of Table 3.

TABLE 5
Bi, Bi/Mn, P, O(1) and O(2) Environments in $Bi_{1.2}Mn_{1.2}PO_{5.5}$ (Distance in Å, Angle in Degree)

Bi and Bi/Mn environments			
Bi(1)–O(1)	2.299(1) (2 ×)	Bi/Mn(1)–O(2)	2.159(9) (2 ×)
Bi(1)–O(2)	2.243(1) (2 ×)	Bi/Mn(1)–O(4)	2.72(5) (2 ×)
Bi(1)–O(3)	2.68(7)	Bi/Mn(1)–O(4)	2.09(5) (2 ×)
Bi(1)–O(4)	2.76(5)	Bi/Mn(1)–O(5)	2.45(5)
		Bi/Mn(1)–O(6)	2.63(5)
		Bi/Mn(1)–O(7)	2.21(6) (2 ×)
		Bi/Mn(1)–O(8)	2.43(8) (2 ×)
		Bi/Mn(1)–O(8)	2.22(8) (2 ×)
P Environment			
P(1)–O(3)	1.59(8)	P(2)–O(6)	1.53(5)
P(1)–O(4)	1.52(5) (2 ×)	P(2)–O(7)	1.40(7)
P(1)–O(5)	1.37(6)	P(2)–O(8)	1.63(8)
		P(2)–O(9)	1.45(5)
O(3)–P(1)–O(4)	102(3) (2 ×)	O(6)–P(2)–O(7)	112(3)
O(3)–P(1)–O(5)	117(5)	O(6)–P(2)–O(8)	105(4)
O(4)–P(1)–O(4)	127(4)	O(6)–P(2)—O(9)	111(4)
O(4)–P(1)–O(5)	105(3) (2 ×)	O(7)–P(2)—O(8)	118(5)
		O(7)–P(2)—O(9)	106(5)
		O(8)–P(2)—O(9)	103(5)
O(1) Environment			
O(1)–Bi(1)	2.299(1) (4 ×)		
$Bi(1)^{i}$–O(1)–$Bi(1)^{ii}$	107.51(3)	$Bi(1)^{ii}$–O(1)–$Bi(1)^{iii}$	105.20(3)
$Bi(1)^{i}$–O(1)–$Bi(1)^{iii}$	115.91(3)	$Bi(1)^{ii}$–O(1)–$Bi(1)^{iv}$	115.91(3)
$Bi(1)^{i}$–O(1)–$Bi(1)^{iv}$	105.20(3)	$Bi(1)^{iii}$–O(1)–$Bi(1)^{iv}$	107.51(3)
O(2) Environment			
O(2)–Bi(1)	2.249(9) (2 ×)		
O(2)–Bi/Mn(1)	2.159(9) (2 ×)		
$Bi(1)^{i}$–O(2)–$Bi(1)^{iv}$	109.0(2)	$Bi(1)^{iv}$–O(2)–$Bi/Mn(1)^{v}$	103.6(2)
$Bi(1)^{i}$–O(2)–$Bi/Mn(1)^{v}$	117.6(3)	$Bi(1)^{iv}$–O(2)–$Bi/Mn(1)^{vi}$	117.6(3)
$Bi(1)^{i}$–O(2)–$Bi/Mn(1)^{vi}$	103.6(3)	$Mn(2)^{v}$–O(2)–$Bi/Mn(1)^{vi}$	106.1(3)

Note. Symmetry code i: x, y, z; ii: $-x,-y,-z$; iii: $-x, y, \frac{1}{2}-z$; iv: $x, -y, \frac{1}{2}-z$; v: $\frac{1}{2}-x, \frac{1}{2}-y, \frac{1}{2}+z$; vi: $\frac{1}{2}-x, y-\frac{1}{2}, -z$.

DISCUSSION AND STRUCTURAL RELATIONSHIPS

Assuming a sum of occupancies for the phosphorus sites equal to one and in accordance with the oxidation state +3 for the Bi atoms and +2 for the M atoms (justified by the preparation of the Zn compound), the formula deduced from the crystal structure approaches is close to $Bi_{1.2}M_{1.2}PO_{5.5}$ with $Z = 8$ formula unit per cell. The formula can also be written as $BiMP_{0.833}O_{4.583}$ very close to the already published $BiCoPO_5$ formula compound (13, 22). Several experiments seem to confirm the proposed formula.

Single phase preparation: First, in the Bi–Mn–P–O system, samples of various compositions were prepared by solid-state reaction according to the experimental section process. A pure phase characterized by its X-ray powder diffraction was only obtained for the Bi:Mn:P = 1:1:0.85 ratio. For all the other prepared compositions it was accompanied by nonidentified impurities. In the same way, several samples of the Bi–Co–P–O system, between $BiCoPO_5$ and $BiMP_{0.833}O_{4.583}$ were examined, and the X-ray powder patterns show systematically the superposition of those of the two limit compounds. The lattice parameters for all the preparations are constant, so we could conclude that the phases have a fixed composition; however, the crystal structure results augur possible weak variations. The X-ray patterns obtained for the three compositions $Bi_{1.2}M_{1.2}PO_{5.5}$ for M = Mn, Co, Zn are totally indexed with the unit cell deduced from the single-crystal study and allow the refinement of lattice parameters. They were refined from powder XRD pattern deconvolution using the program Profile from the Siemens Diffrac/AT package (23) and are reported in Table 4 with the corresponding figures of merit (24). For the three compounds, the measured densities are in good agreement with the calculated values assuming eight units $Bi_{1.2}M_{1.2}PO_{5.5}$ per cell (Table 4). Complete solid solutions were obtained between two compounds. For example, the variation of the unit cell parameters for the $Bi_{1.2}(Mn_{1-x}Co_x)_{1.2}PO_{5.5}$ solid solution is shown in Fig. 2, in agreement with the discussion that the a parameter regularly decreases while the b and c parameters remain practically constant.

EDS measurement: Several EDS analyses performed on $Bi_{1.2}Mn_{1.2}PO_{5.5}$ single crystals show homogeneous results and confirm the formulae (average: exp./calc. atomic %: Bi 35.9/35.0, Mn 35.0/35.0, P 29.1/30.0).

Magnetic properties: Thermal magnetic susceptibilities and inverse susceptibilities are shown in Fig. 3a for the manganese and cobalt compounds. For the manganese compound, the experimental data can be fitted above 30 K with a Curie–Weiss law, $\chi = C/(T - \theta)$, with a Weiss temperature $\theta = -62$ K. The negative value of θ and the monotonical decrease of χT (Fig. 3b) with a lowering of temperature reveal the presence of AF interactions between the metallic cations at low temperature. The value of $p_{\text{eff}} = 5.91\,\mu B/Mn$ deduced from the paramagnetic domain is in good accordance with the calculated value ($p_{\text{eff}} = 5.91\,\mu B$) assuming a spin-only Mn^{2+} contribution and the formula $Bi_{1.2}M_{1.2}PO_{5.5}$ with $Z = 8$ formula unit per cell.

For the cobalt compound the same type of behavior is observed with $\theta = -42$ K, and the calculated value of $p_{\text{eff}} = 5.06\,\mu B/Co$ is largely superior to the spin-only $S = \frac{3}{2}$ approximation between the calculated values for a spin only contribution ($p_{eff} = 3.87\,\mu B$). It is well known that Co^{2+} cation with ground-state quantum term $^4F_{9/2}$ shows a

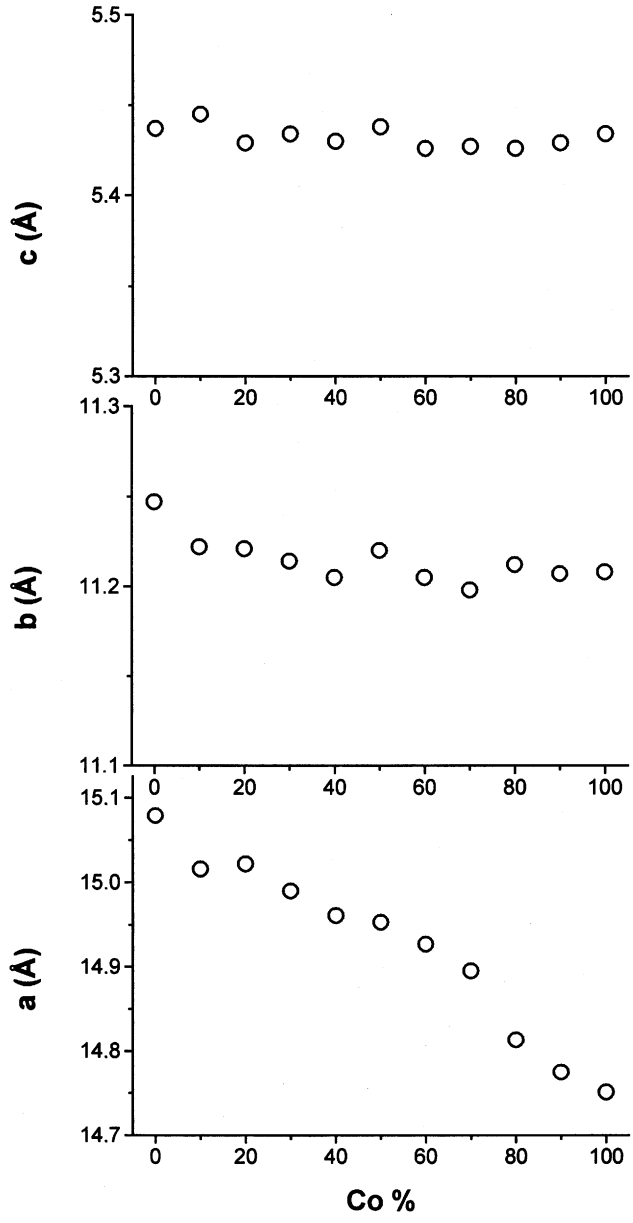

FIG. 2. Lattice parameters variation versus x for the $Bi_{1.2}(Mn_{1-x}Co_x)_{1.2}PO_{5.5}$ solid solution ($0 \le x \le 1$).

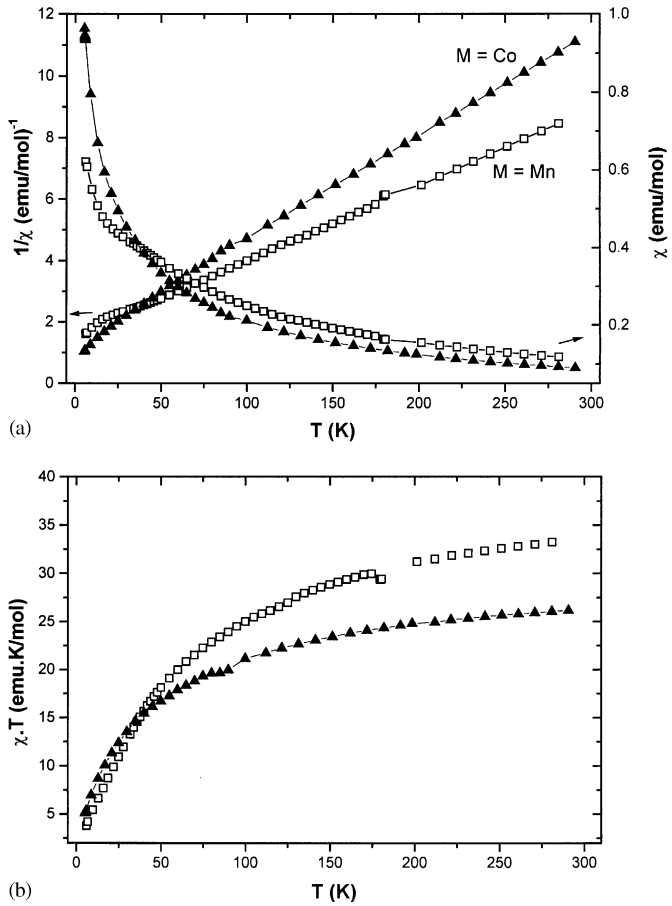

FIG. 3. Thermal evolution of the magnetic susceptibility for $Bi_{1.2}M_{1.2}PO_{5.5}$ (M = Mn, Co) compounds: (a) variation of χ and $1/\chi$ versus T and (b) variation of the χT product versus T.

large spin–orbit coupling and lies in the 4.4–5.2 μB/cation. In that case the effective moment can be calculated on the basis of small multiplet widths $p_{\text{eff}} = [L(L+1)+4(S)(S+1)]^{1/2} = 5.20\,\mu B$ in agreement with experimental results.

For both materials the susceptibilities slightly deviate from the Curie–Weiss law under 40 K, probably imaging the setting randomly depleted antiferromagnetic couplings because of partial occupancies of M sites.

Due to the high disorder affecting both the metallic atoms, the phosphorus and the oxygens, it is very difficult to describe the anionic environment of the cations and to describe the structure framework from the linkage of cation-centered coordination polyhedra through corners, edges and/or faces, as commonly realized. At least, phosphorus is likely to be located at the center of tetrahedra that appear strongly distorted because of the inaccuracy of several oxygen coordinates due to disorder (Table 5). However, Bi(1) atom and the oxygen atoms O(1) and O(2) which do not belong to phosphate groups are perfectly localized, and we shall demonstrate that these atoms are the basis of the building of mono-dimensional ribbons of three tetrahedra width. This crystallographic new description is based on the simple observation of the lacunar fluorite type δ-Bi_2O_3 crystal structure. The δ form of Bi_2O_3 is stable only between 729°C and 840°C (melting point) but can be stabilized by adding several cations (25–28) and provides the simplest example of a tri-dimensional infinite cluster of edge-sharing tetrahedra (Fig. 4). It is built from $\frac{3}{4}$ of oxygen-centered and $\frac{1}{4}$ of empty Bi_4 edge-sharing tetrahedra with Bi–O distances of 2.45 Å.Thus, a wide range of recently studied materials were re-analyzed on the basis of oxygen-centered polyhedra and appear to exhibit a network built from one-dimensional ribbons of different width providing evidences of a structural relation between the compounds.

Clusters of OBi_4 Tetrahedra

$Bi_3M_3O_{11}$ Considering the notion of infinite OBi_4 clusters of δ-Bi_2O_3, it is noteworthy that dense associations of OBi_4 tetrahedra can be found fit into a metal–oxygen framework. For instance, in $Bi_3Ru_3O_{11}$ (29), clusters built from four edge-shared OBi_4 tetrahedra occupy the voids of the $Ru_{12}O_{36}$ tri-dimensional framework of edge- and corner-shared RuO_6 octahedra, so the compound can be considered as $2Bi_6O_4^{10+}$, $Ru_{12}O_{36}^{20-}$ (Fig. 5a). This structure, related to that of cubic $KSbO_3$ (30), is also found for phases with compositions $Bi_3Os_3O_{11}$, $Bi_3Pt_3O_{11}$ (31) and $Bi_3GaSb_2O_{11}$ (32). Astonishingly, while isolated OLa_4 tetrahedron occupies the voids of a similar framework to

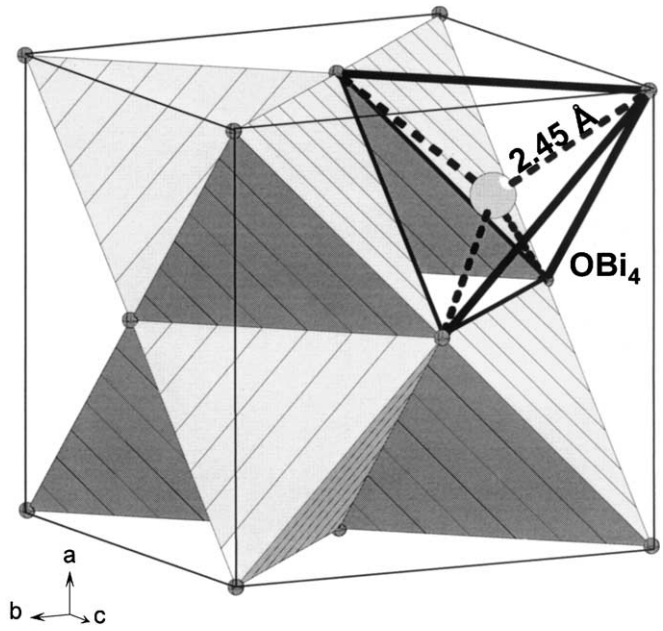

FIG. 4. Fluorite-type structure of δ-Bi_2O_3 showing the unit cell in terms of OBi_4 and Bi_4 tetrahedra.

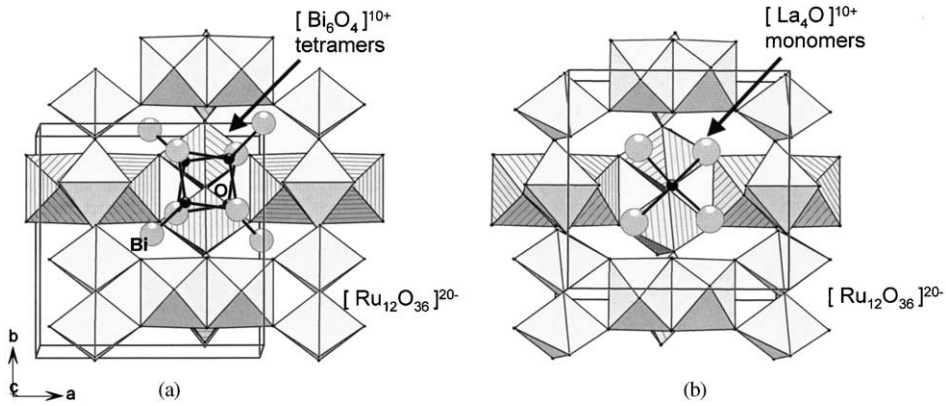

FIG. 5. Occupation of the large cavity of the $Ru_{12}O_{36}$ octahedral network by (a) one O_4Bi_6 cluster built from edge-shared OBi_4 tetrahedra in $Bi_3Ru_3O_{11}$ and (b) one La_4O tetrahedron in $La_4Ru_6O_{19}$.

form $La_4Ru_6O_{19}$ ($2La_4O^{10+}$, $Ru_{12}O_{36}^{20-}$), Fig. 5b (33), isolated tetrahedron OBi_4 cannot be stabilized within this framework and till today the synthesis of $Bi_4Ru_6O_{19}$ has not been achieved. Their existence would provide the smallest building unit of the edifices to be described.

Monodimensional Chains

$BiMPO_5$. The synthesis and the crystal structure of $BiNiPO_5$ and $BiCoPO_5$ have been recently reported (12, 13, 22). The crystal structure of these compounds has been first described in terms of mixed double chains of two edge-sharing MO_6 octahedra alternating with two edge-sharing BiO_6 octahedra and connected to each other through the PO_4 tetrahedra to form a three-dimensional network (12). Another description enhances the role of Bi^{3+} ions located in large tunnels formed by a complex tri-dimensional assembly of M_2O_{10} dimers linked by PO_4 groups (13). Therefore, these compounds are oxy-phosphates and can be formulated $BiMO(PO_4)$; the highlighted oxygen atom that does not participate in the formation of the PO_4 entity is tetrahedrally coordinated by four metal atoms, two bismuth and two M atoms (Fig. 6a). The OBi_2M_2 tetrahedra share opposite Bi–Bi and M–M edges to form $(OBiM)^{3+}$ one-dimensional chains running along the c-axis of the monoclinic cell, and the value of the c parameter is twice the height of one tetrahedron, that is to say about 5.2 Å. The PO_4^{3-} anions are located between the chains (Fig. 6b).

Similar columns built from OBi_2Pb_2 and OPb_4 tetrahedra are found in $BiPbXO_5$ (X = P, V, As) and Pb_2SO_5 ($PbPbO(SO_4)$), respectively (15). The description enables the evidence of the close relation between both crystal structures despite a cell doubling and a symmetry lowering

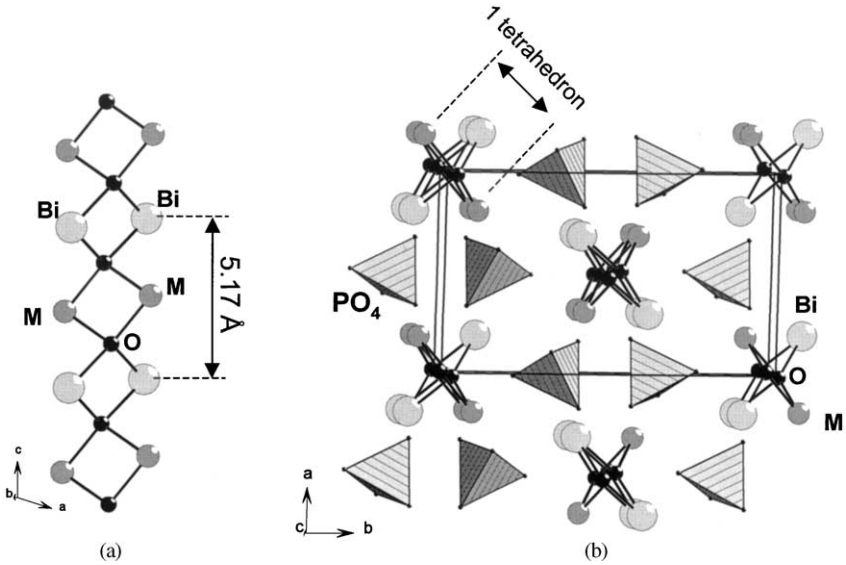

FIG. 6. (a) The one tetrahedron large mono-dimensional chain in $BiMPO_5$ (M = Ni, Co) compounds running along the c-axis of the monoclinic unit cell and (b) the crystal structure viewed along the [001] direction showing the arrangement of $(OBiM)^{3+}$ chains and PO_4^{3-} groups.

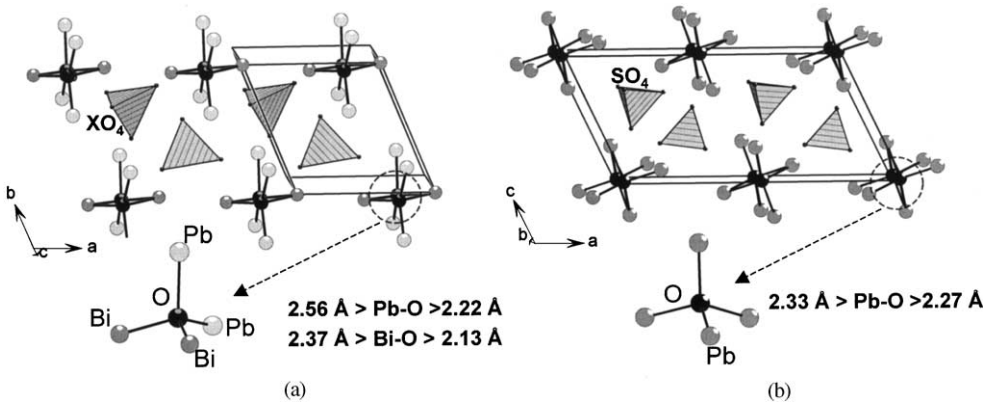

FIG. 7. Comparison of the crystal structure of (a) $BiPbXO_5$ (X = P, V, As) and (b) Pb_2SO_5.

from the monoclinic Pb_2SO_5 to the triclinic $BiPbXO_5$ materials, Fig. 7a and 7b.

Bi_2MO_{5-x}: One-dimensional chains formed from OBi_4 tetrahedra linked by opposite edges exist in Bi_2AuO_5 (34). The OBi_2^{2+} chains are located between columns resulting from the stacking of AuO_4 square planes, Fig. 8a and 8b. A similar arrangement is encountered in Bi_2CuO_4 (35) and related materials (36), but with empty Bi_4 tetrahedra.

Association of chains in columns, ribbons, and layers

$Bi_{26}Mo_{10}O_{69}$. In this compound, very dense columnar clusters are formed from edge sharing between five crystallographically independent oxygen-centered OBi_4 tetrahedra (37,38). These clusters can be regarded as two crossed ribbons three tetrahedra wide sharing their central tetrahedron, Fig. 9. Therefore, our model does not consider particular oxygen atoms located around the column, at the center of OBi_3 triangular planes, Bi–O = 2.2 Å. The columns extending along the twofold axis of the monoclinic cell display a clear covalent character and are connected by MoO_4 tetrahedra. Other bismuth atoms are also located between the columns. Variation of the content of these inter-column bismuth leads to the preparation of a solid solution that extends from $Bi_{25.75}Mo_{10}O_\delta$ to $Bi_{27.75}Mo_{10}O_\delta$ on the Bi_2O_3–MoO_3 line (37). Similar columns are found in $Bi_{13}Mo_4VO_{34}$ (39), in the high-temperature form of Bi_2MoO_6 (40) and in the recently published $Bi_6Cr_2O_{15}$ (41).

BiM_2XO_6. Numerous compounds with the formula $Bi^{III}M_2^{II}XO_6$ (M = Mg, Ca, Cu, Cd, Pb; X = P, V, As) have been reported (1–9,11,14,16). Note that their unit cells (orthorhombic, $a \sim 11.5$ Å, $b \sim 5.2$ Å, $c \sim 7.8$ Å) show two parameters common to $Bi_{1.2}M_{1.2}PO_{5.5}$. The description useful to investigate the magnetic properties of magnetic metal-containing compounds such as $BiCu_2PO_6$ is to

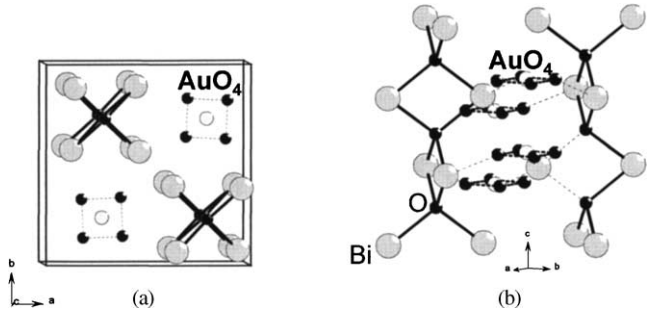

FIG. 8. (a) Projection along the c-axis of the tetragonal unit cell and (b) perspective view showing the $(OBi_2)^{4+}$ chains and the columnar stacking of AuO_4 squares in Bi_2AuO_5.

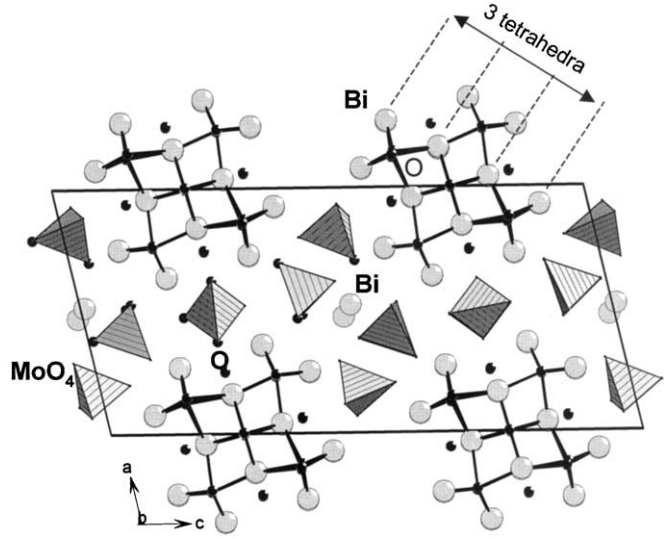

FIG. 9. Projection of the $Bi_{26}Mo_{10}O_{69}$ structural model on the (010) plane of the monoclinic cell showing the $Bi_{12}O_{14}$ columns running along the b-axis. The MoO_4 groups and some Bi atoms are disordered in the space between the columns.

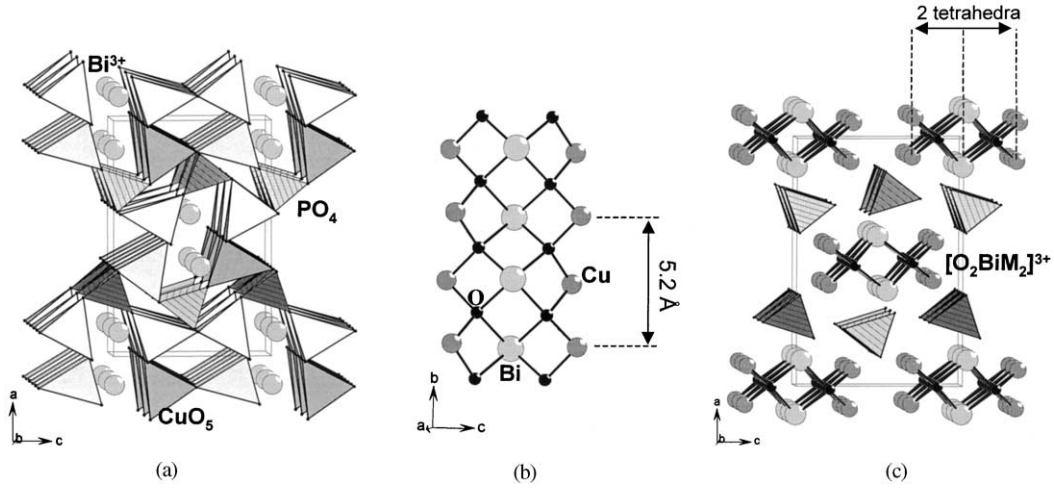

FIG. 10. The crystal structure of $BiCu_2PO_6$ showing (a) the linkage of CuO_5 and PO_4 polyhedra and interspersed Bi^{3+} ions, (b) the two tetrahedra width ribbon in BiM_2PO_6 compounds and (c) the projection of the structure along the [010] direction showing the arrangement of $(O_2BiM_2)^{3+}$ chains and PO_4^{3-} groups.

consider $[M_2O_8]$ or $[M_2O_{10}]$ double chains built from MO_5 square pyramids or MO_6 octahedra depending on the nature of M and with charge balance provided by interspersed Bi^{3+} cations, Fig. 10a. Generally, these compounds are also oxy-phosphates and can be formulated $BiM_2O_2(PO_4)$. Considering the strong M environment differences existing among this wide materials series (14), a common description based on the oxygen atoms that does not participate in the formation of the PO_4 entity is likely and very informative. They are, as in $BiMPO_5$ compounds, tetrahedrally coordinated by four metal atoms, two bismuth and two M atoms. One tetrahedron shares opposite Bi–M edges with two other tetrahedra to form infinite OBi_2M_2 columns, and two columns related by an inversion center share all their Bi–Bi edges to form a double chain of formula $(O_2BiM_2)^{3+}$, Fig. 10b. The unit cell parameter is once again close to 5.2 Å, twice the height of one tetrahedron. Each tetrahedron shares three edges with other tetrahedra. The obtained double chains are parallel to each other and connected by PO_4 tetrahedra (Fig. 10c). Sheets of double chains and PO_4 entities parallel to the (100) plane alternate along the a direction of the orthorhombic unit cell (Fig. 10c).

$Bi_4Cu_3X_2O_{14}$. The structure of the corresponding oxy-phosphate (11) is similar to that of the oxy-vanadate analog $Bi_4Cu_3P_2O_{14}$ (42). It can be described from triple chains of edge-sharing oxygen-centered tetrahedra. The building block of these chains is constituted of one central

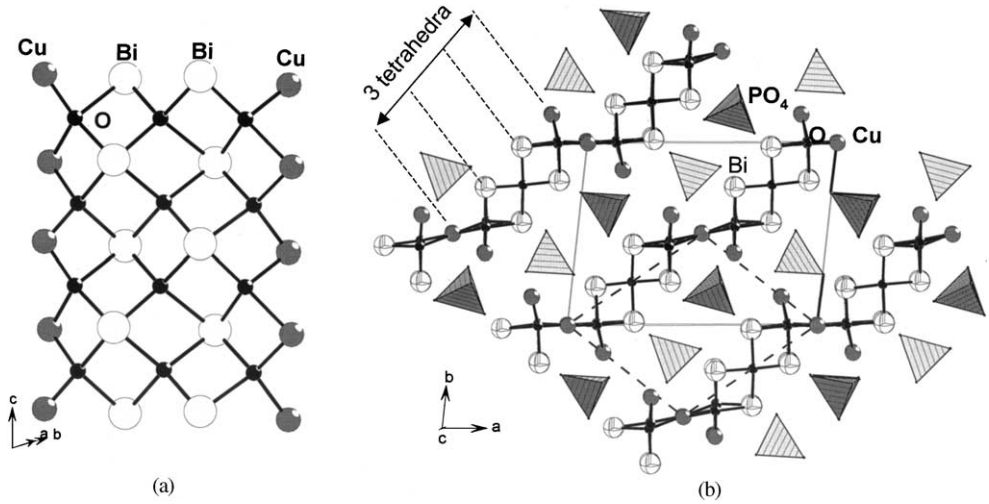

FIG. 11. (a) The three tetrahedra width ribbon in $Bi_4Cu_3X_2O_{14}$ (X = P, V) compounds and (b) the projection of the structure along the [001] direction showing the linkage of the ribbons through Cu atoms to form $(O_3Bi_2Cu_{1.5})^{3+}$ layers connected by PO_4^{3-} groups.

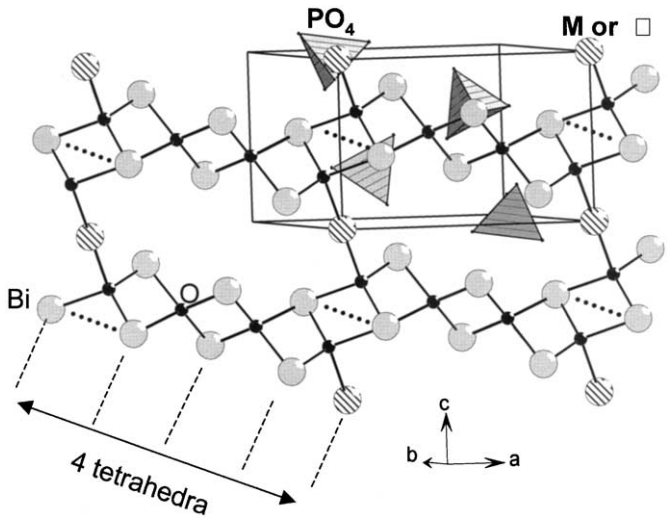

FIG. 12. Tetrahedral tetramers connected by edges and corners in $Bi_{6.67}(PO_4)_4O_4$.

OBi_4 tetrahedron flanked on each part with one OBi_2Cu_2 tetrahedron. The trimeric units $O_3Bi_4Cu_4$ share their Bi–Bi and Bi–*M* edges to form the triple chains. The triple chains are not isolated; they are connected by terminal copper atoms to constitute crenel layers of formula $(O_3Bi_2Cu_{1.5})^{3+}$ which alternate with PO_4 sheets (Fig. 11).

$Bi_{6+x}M_y(XO_4)O_4$. These series (17) display the cases of tetrahedral tetramers. Two central OBi_4 and two terminal $OMBi_3$ tetrahedra constitute the segments by sharing edges. In $Bi_{6.67}(PO_4)_4O_4$, *M* is Bi^{3+} (occupancy $\frac{2}{3}$) or a vacancy (occupancy $\frac{1}{3}$) while it can guest several *M* chemical nature in $Bi_{6+x}M_y(PO_4)O_4$ ($M = Sr^{2+}$, Cd^{2+}, Ca^{2+}, Pb^{2+}, Li^+, Na^+, K^+). These compounds, at least, show the possibility for the end of chains to adopt vacancies while the central oxygens remain fully coordinated by bismuth cations. As previously observed in $Bi_4Cu_3X_2O_{14}$, the ribbons interconnect to each other by sharing terminal adjacent edges, so forming infinite crenel-like chains. The *M* corners are shared by the chains to form infinite 2-D layers (Fig. 12).

$Bi_{1.2}M_{1.2}PO_{5.5}$ compounds. In the structure of the presently studied compounds, the oxygen atom O(1) is tetrahedrally coordinated by four Bi(1) bismuth atoms (Table 5). As in $Bi_4Cu_3P_2O_{14}$, the central $O(1)Bi(1)_4$ tetrahedron is also flanked on each part by two tetrahedra with the formula $O(2)Bi(1)_2Bi(2)_2$, $O(2)Bi(1)_2Bi(2)Mn(1)$ or $O(2)Bi(1)_2Mn(1)_2$ depending on the occupation of the corresponding (8*j*) site either by Bi(2) or Mn(1) atom to form a trimeric building block. The obtained trimeric units share their Bi–Bi and Bi–*M* edges to form a ribbon of three tetrahedra width running along the *c*-axis of the orthorhombic unit cell (Fig. 13). The successive ribbons lie parallel to the (010) plane, so two lattice parameters are approximately common with the lattice of $BiMPO_5$ and BiM_2PO_6 compounds described above: the *c* parameter, 5.2–5.3 Å, which corresponds to the height of two edge-shared tetrahedra and the *b* parameter, 11–12 Å, which is twice the distance between two sheets of ribbons. The third parameter depends on the ribbon widths, on their arrangement and on the inter-layer content. In $Bi_{\sim 1.2}M_{\sim 1.2}PO_{5.5}$ compounds, the space between the ribbons is occupied not only by PO_4 groups but also by *M*(2) atoms; these groups and atoms are both highly disordered. This disorder is a direct consequence of the mixed occupancy of the extremities of the triple chains but

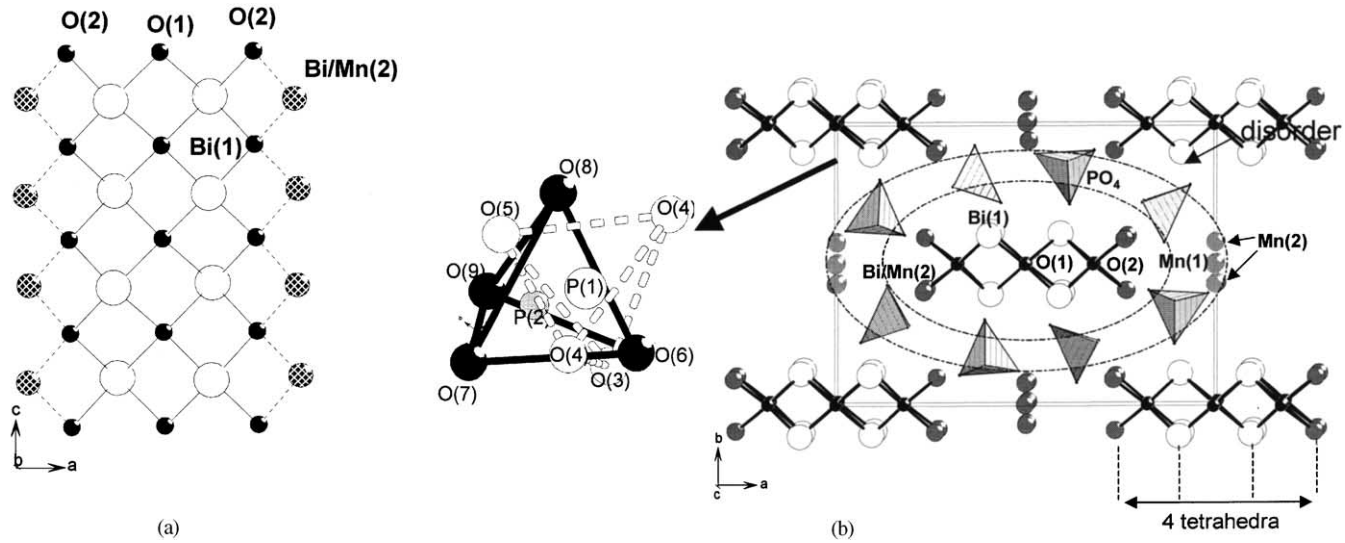

FIG. 13. (a) The three tetrahedra width ribbon in $Bi_{1.2}M_{1.2}PO_{5.5}$ (M = Mn, Co, Zn) compounds and (b) the projection of the structure along the *c*-axis of the orthorhombic cell showing the high disorder of PO_4^{3-} groups and M^{2+} ions in the inter-ribbon space.

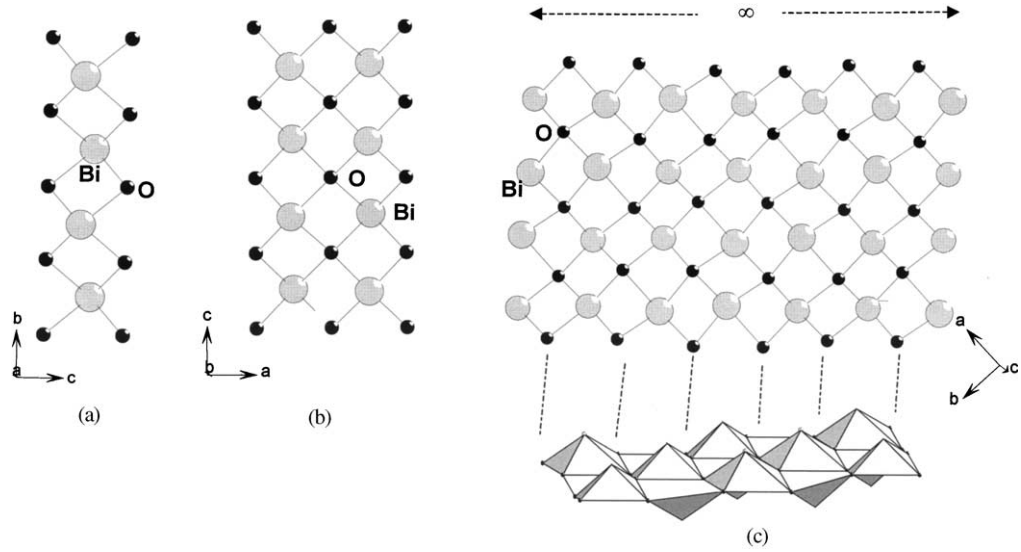

FIG. 14. From (a) the BiO_2^- chain in the BiM_2PO_6 compounds to (c) the $Bi_2O_2^{2+}$ layer in the Aurivillius phases; (b) the intermediate Bi_2O_3 ribbons common to $Bi_4Cu_3X_2O_{14}$ (X = P, V) and $Bi_{1.2}M_{1.2}PO_{5.5}$ compounds.

can also be due to the larger space between triple chains than between single or double chains. While the single and double chains are surrounded by six phosphate groups, the triple chains are surrounded by eight groups leading to different PO_4/chains ratio, 1 and 2, respectively.

It is necessary to notice that only the positions at the border of the ribbons are occupied by M atoms. In other words, in double and triple chains the central tetrahedron atoms are necessarily bismuth atoms. They have very characteristic environments with four short distances to oxygen atoms at the same side of the bismuth atom (Table 5). Actually in ribbons of two or three tetrahedra width, the oxygen atoms are at the corners of squares and the bismuth atoms are at the perpendicular of the center alternatively above and below the oxygen plane. Thus the bismuth and oxygen atoms form a $[BiO_2]^-$ chain in the BiM_2PO_6 compounds and a $[Bi_2O_3]$ double chain in $Bi_4Cu_3P_2O_{14}$. The same situation is present in the $[Bi_2O_2]^{2+}$ layers of the Aurivillius phases, and in these large family of compounds, the oxygen atoms of the layers are all tetrahedrally coordinated by bismuth atoms. These layers can be considered the infinite extension of edge-shared tetrahedra ribbons (Fig. 14).

Toward Ribbons of Superior Width or toward Other Arrangements

The several compounds found with the formula $Bi^{III}M_2^{II}XO_6$ (X = As, P, V; M = Mg, Ca, Cu, Cd, Pb) adopt the same structural arrangement with the same orthorhombic unit cell; however, slight distortions lead to different space groups, i.e., *Pnma*, *Bbmm*, *Bb2$_1$m*, using the $a \approx 11.5$ Å, $b \approx 5.7$ Å, $c \approx 7.8$ Å unit cell orientation. For example, the crystal structure of $BiCd_2PO_6$ has been refined in the *Bbmm* space group (8) and that of $BiZn_2PO_6$ in the *Pnma* space group; however, this compound undergoes a P to B phase transition at about 325°C (14). We began a study of the intermediate phases between these two compounds and we are going to present the first results of the investigation of the $BiZn_{2-x}Cd_xPO_6$ system. Figure 15a shows the X-ray

TABLE 6
Unit Cell Parameters for the $BiZn_{2-x}Cd_xPO_6$ Compounds

x	a (Å)	b (Å)	c (Å)	V (Å^3)	Lattice	F (20)
0	11.897(2)	5.277(1)	7.819(2)	490.9	P	45(0.0100, 67)[a]
0.5	11.307(4)	5.428(3)	15.089(8)	926.1	I	21(0.0128, 75)
1	11.590(2)	5.489(2)	23.250(5)	1479.1	A	38(0.0094, 56)
1.5	12.020(3)	5.371(2)	8.342(2)	538.5	B	70(0.0080, 36)
2	11.944(1)	5.374(1)	8.505(1)	545.9	B	44(0.0062, 73)

[a] F(30).

TABLE 7
Unit Cell Parameters for the $BiMCdPO_6$ (M = Ni, Co, Zn, Cu) Compounds

M	a (Å)	b (Å)	c (Å)	V (Å^3)	Lattice	F (20)
Ni	11.346(3)	5.494(2)	15.316(4)	954.7	I	65(0.0075, 41)
Co	11.556(3)	5.485(1)	23.327(5)	1478.6	A	58(0.0091, 38)
Zn	11.590(5)	5.489(2)	23.250(5)	1479.1	A	38(0.0094, 56)
Cu	11.544(5)	5.443(2)	38.574(21)	2423.8	P	19(0.0179, 61)

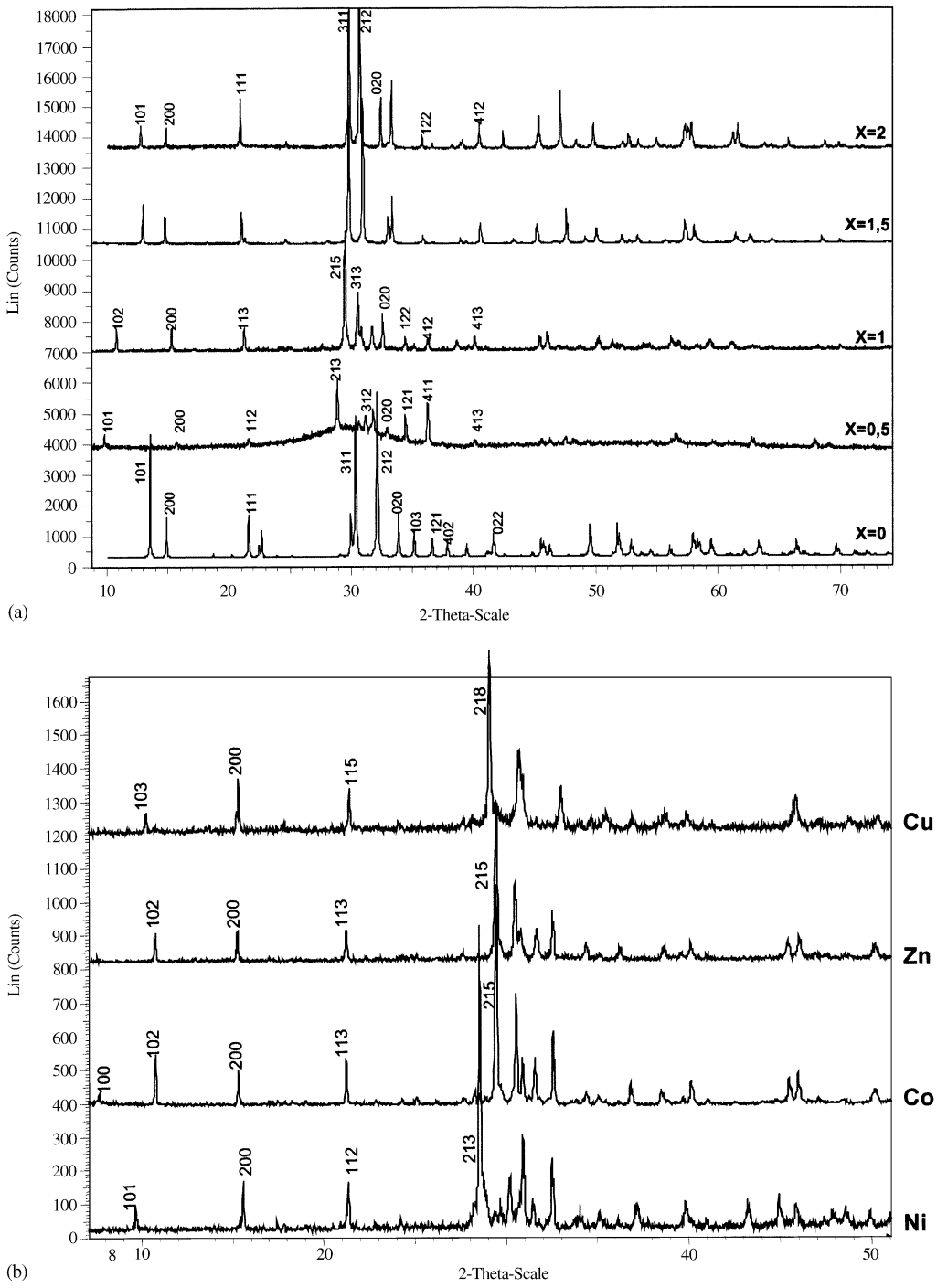

FIG. 15. X-ray powder diffraction patterns for (a) $BiZn_{2-x}Cd_xPO_6$ ($x = 0$, 0.5, 1.0, 1.5 and 2.0) compounds and (b) BiMCdPO$_6$ (M = Ni, Co, Zn, Cu) compounds.

patterns obtained for $x = 0$, 0.5, 1.0, 1.5, and 2. While the X-ray pattern for $x = 1.5$ can be indexed with the same unit cell as that of $BiCd_2PO_6$, the patterns for $x = 0.5$ and 1.0 are different. They are unambiguously indexed in orthorhombic lattices with similar a and b parameters (characteristic of the distances between ribbons and of the height of two edge-shared tetrahedra) but with different c parameters; extinctions of hkl reflections indicated the lattice symmetries reported in Table 6. On the other hand, the study of the compositions BiMCdPO$_6$ for M = Co, Ni,

Cu, Zn indicates different c parameter values and lattice symmetries (Fig. 15b and Table 7). For $M = Ni$ and for $BiZn_{1.5}Cd_{0.5}PO_6$ the unit cell is close to that obtained for the compounds $Bi_{\sim 1.2}M_{\sim 1.2}PO_{5.5}$ ($M = Mn$, Co, Zn) reported in this paper.

In view of the lattice parameters one could think that the unit cells for the different compounds are super-cells of the basic cell adopted by the simple BiM_2PO_6 compounds with a multiplication of the c parameter (≈ 7.8 Å) by 2 (≈ 15.2 Å), 3 (≈ 23.3 Å), 4 (no example) and 5 (≈ 38.6 Å). Actually, the XRD patterns are strongly modified from one compound to another avoiding any common sublattice reminiscence. Furthermore, the study of the $Bi_{1.2}M_{1.2}PO_{5.5}$ compounds showed that it had nothing of it and we can rather imagine wider ribbons or the coexistence of ribbons of different widths in the same structure. In spite of numerous difficulties (disorders, lack of single-crystal, etc.) we hope that the structures of these compounds can be discussed soon in forthcoming reports.

As for the presently studied compounds, the crystal structure determination of some of the above-described compounds presents various difficulties, for example, in $Bi_4V_2O_{11}$ (43), the parent compound of the BIMEVOX family (44), the vanadium and the oxygen atoms between the perfectly localized Aurivillius type $(Bi_2O_2)^{2+}$ layers are highly disordered (45), it is the same for the atoms of bismuth and oxygen between the columns in the $Bi_{26}Mo_{10}O_{69}$ type compounds, ternary bismuth-rich compounds with fluorite-related structures display a variety of superstructures and/or commensurate and incommensurate modulations (46–50). All these compounds are among the best oxygen ion conductors known (51). Such properties can be hoped for the disordered bismuth-based oxy-phosphates presented in this paper and those to come.

ACKNOWLEDGMENTS

The authors sincerely acknowledge Dr. Marielle Huvé, Ouassila Mebarki and Marie Colmont from LCPS, Villeneuve d'Ascq, France, for technical support.

REFERENCES

1. J. Huang and A. W. Sleight, *J. Solid State Chem.* **100,** 170 (1992).
2. J. Huang, Q. Gu, and A. W. Sleight, *J. Solid State Chem.* **105,** 599 (1993).
3. I. Radosavljevic, J. S. O. Evans, and A. W. Sleight, *J. Solid State Chem.* **137,** 143 (1998).
4. I. Radosavljevic, J. S. O. Evans, and A. W. Sleight, *J. Solid State Chem.* **141,** 149 (1998).
5. I. Radosavljevic, J. S. O. Evans, and A. W. Sleight, *J. Alloys Compd.* **284,** 99 (1999).
6. I. Radosavljevic and A. W. Sleight, *J. Solid State Chem.* **149,** 143 (2000).
7. F. Abraham, M. Ketatni, G. Mairesse, and B. Mernari, *Eur. J. Solid State Chem.* **31,** 313 (1994).
8. N. Tancret, Ph.D. Dissertation, Université des Sciences et Technologies de Lille, France, Septembre 1995.
9. A. Mizrahi, J. P. Wignacourt, and H. Steinfink, *J. Solid State Chem.* **133,** 516 (1997).
10. A. Mizrahi, J. P. Wignacourt, M. Drache, and P. Conflant, *J. Mater. Chem.* **5,** 901 (1995).
11. M. Ketatni, Ph.D. Dissertation, Université des Sciences et Technologies de Lille, France, April 1995.
12. F. Abraham and M. Ketatni, *Eur. J. Solid State Inorg.* Chem. **32,** 429 (1995).
13. M. Ketatni, F. Abraham, and O. Mentre, *Solid State Sci.* **1,** 449 (1999).
14. M. Ketatni, B. Mernari, F. Abraham, and O. Mentre, *J. Solid State Chem.* **153,** 48 (2000).
15. S. Giraud, A. Mizrahi, M. Drache, P. Conflant, J. P. Wignacourt, and H. Steinfink, *Solid State Sci.* **3,** 593 (2001).
16. I. Radosavljevic, J. A. K. Howard, R. L. Withers, and J. S. O. Evans, *Chem. Commun.* **19,** 1984 (2001).
17. M. Ketatni, O. Mentre, F. Abraham, F. Kzaiber, and B. Mernari, *J. Solid State Chem.* **139,** 274 (1998).
18. J. De Meulenaer and H. Tompa, *Acta Crystallogr.* **19,** 1014 (1965).
19. "International Tables for X-ray Crystallography," Vol. IV. Kynoch Press, Birmingham, UK, 1974.
20. D. T. Cromer and D. Liberman, *J. Chem. Phys.* **53,** 1891 (1970).
21. C. T. Prewitt, "SFLS-5, Report ORNL-TM 305." Oak Ridge National Laboratory, Oak Ridge, TN, 1966.
22. S Nadir, J. S. Swinnea, and H. Steinfink, *J. Solid State Chem.* **148,** 295 (1999).
23. A. W. Visser, *J. Appl. Crystallogr.* **2,** 89 (1969).
24. G. S. Smith and R. L. Snyder, *J. Appl. Crystallogr.* **12,** 60 (1979).
25. P. Conflant, J. C. Boivin, and D. Thomas, *J. Solid State Chem.* **18,** 133 (1976).
26. T. Takahashi, T. Esaka, and H. Iwahara, *J. Appl. Electrochem.* **5,** 197 (1975).
27. M. J. Verkerk and A. J. Burgraaf, *Solid State Ionics* **3/4,** 463 (1981).
28. A. Watanabe and T. Kikuchi, *Solid State Ionics* **21,** 287 (1986).
29. F. Abraham, D. Thomas, and G. Nowogrocki, *Bull. Soc. Fr. Minéral. Cristallogr.* **98,** 25 (1975).
30. P. Spiegelberg, *Arkiv. Kemi* **14A,** 1 (1940).
31. A. W. Sleight, *Mater. Res. Bull.* **9,** 1177 (1974).
32. A. W. Sleight and R. J. Bouchard, *Inorg.Chem.* **12,** 2314 (1973).
33. F. Abraham, J. Tréhoux, and D. Thomas, *Mater. Res. Bull.* **12,** 43 (1977).
34. J. Geb and M. Jansen, *J. Solid State Chem.* **122,** 364 (1996).
35. P. Conflant, J. C. Boivin and D. Thomas, *Rev. Chem. Miner.* **14,** 249 (1977).
36. N. Henry, O. Mentré, J.C. Boivin and F. Abraham, *Chem. Mater.* **13,** 543 (2001).
37. R. N. Vannier, G. Mairesse, F. Abraham, and G. Nowogrocki, *J. Solid State Chem.* **122,** 394 (1996).
38. D. J. Buttrey, T. Vogt, G. P. A. Yap, and A. L. Rheingold, *Mater. Res. Bull.* **32,** 947 (1997).
39. R. Enjalbert, G. Hasselmann, and J. Galy, *J. Solid State Chem.* **131,** 236 (1997).
40. D. J. Buttrey, T. Vogt, U. Wildgruber, and W. R. Robinson, *J. Solid State Chem.* **111,** 118 (1994).
41. J. Grins, S. Esmaeilzadeh, and S. Hull, *J. Solid State Chem.* **163,** 144 (2002).
42. G. B. Deacon, B. M. Gatehouse, and G. N. Ward, *Acta Crystallogr. C* **50,** 1178 (1994).

43. F. Abraham, M.F. Debreuille-Gresse, G. Mairesse, and G. Nowogrocki, *Solid State Ionics* **28–30,** 529 (1988).
44. F. Abraham, J. C. Boivin, G. Mairesse, and G. Nowogrocki, *Solid State Ionics* **40–41,** 934 (1991).
45. R. N. Vannier, G. Mairesse, F. Abraham and G. Nowogrocki, *J. Solid State Chem.* **103**, 441 (1993).
46. W. Zhou, *J. Solid State Chem.* **87,** 44 (1990).
47. W. Zhou, *J. Solid State Chem.* **101,** 1 (1992).
48. C. D. Ling, R. L. Withers, S. Schmid, and J. Thompson, *J. Solid State Chem.* **137,** 42 (1998).
49. M. Valldor, S. Esmaeilzadeh, C. Pay-Gomez, and J. Grins, *J. Solid State Chem.* **152,** 573 (2000).
50. S. Esmaeilzadeh, S. Lundgren, U. Halenius, and J. Grins, *J. Solid State Chem.* **156,** 168 (2001).
51. J. C. Boivin and G. Mairesse, *Chem. Mater.* **10,** 2870 (1998).